53^{rd} AIAA Aerospace Sciences Meeting and Exhibit, 7-10 January 2015, Kissimmee, Florida.

Physical Diffusion Cures the Carbuncle Phenomenon

Joseph M. Powers*
University of Notre Dame, Notre Dame, Indiana, 46556-5637, USA

Jeffery D. Bruns†
University of Notre Dame, Notre Dame, Indiana, 46556-5637, USA

Aleksandar Jemcov‡
University of Notre Dame, Notre Dame, Indiana, 46556-5637, USA

The supersonic flow of a calorically perfect ideal gas past a two-dimensional blunt body was investigated. An unphysical anomaly known as the carbuncle phenomenon has been predicted by earlier studies of this flow that use so-called high resolution schemes which employ flux limiters within shock-capturing methods applied to the Euler equations. As a remedy, this study introduces physical momentum and energy diffusion via a simple discretization of the ordinary Navier-Stokes equations, employed on a sufficiently fine grid to capture viscous shocks. To check if this cures the anomaly, flow over a cylinder of radius $a = 150$ microns of viscous air with freestream Mach number $M_1 = 5.73$, pressure $p_1 = 12.4272$ Pa, and temperature $T_1 = 39.667$ K was simulated. The numerical solution was calculated with first order spatial and fourth order temporal discretizations, and it was seen that physical diffusion, appropriately resolved, removes the carbuncle phenomenon.

I. Introduction

For over two decades, anomalous solutions have been predicted by so-called high resolution schemes which employ flux limiters within shock-capturing methods applied to the Euler equations in simulating the supersonic flow of a gas over a blunt body. This aberration, often described as the "carbuncle phenomenon," was first predicted by Peery and Imlay [1] and has been widely reported in the literature; representative samples include contributions from Quirk, [2] Robinet, et al., [3] Srinivasan, et al., [4] Kitamara, et al., [5] and MacCormack. [6] The carbuncle phenomenon often appears as a high amplitude incongruity in the neighborhood of the shock's axis of symmetry. Dumbser, et al. [7] used a robust matrix stability analysis to demonstrate that above a threshold Mach number M, a wide variety of high resolution schemes applied to the Euler equations display "unconditional instability with exponential error growth," independent of both the time-advancement scheme and chosen Courant-Fredrichs-Lewy (CFL) number. This matrix stability analysis was extended by Chauvat, et al. [8] As the carbuncle phenomenon is not observed in nature, most have hypothesized that it is either an anomaly of the chosen numerical method, or an inadequacy of the underlying mathematical model, with far more attention focused on the former than the latter. Elling [9] has gone so far as to describe the phenomenon as "incurable."

However, a small fraction of studies has recognized that physical diffusion can be offerred as a remedy. Pandolfi and D'Ambrosio [10] considered this but noted for calculations for which the viscous shock was probably under resolved that "even for unpractically low Reynolds numbers, the solution is still affected by the carbuncle." Ismail, et al. [11] considered a viscous cure in passing, but discounted it because the carbuncle "disappears only at very low Reynolds number." Liou [12] also briefly described viscous solutions, but focused on a different approach. Recently, Ohwada, et al. [13] as well as Li, et al. [14] have modeled

*Associate Fellow, AIAA, Professor, Department of Aerospace and Mechanical Engineering. powers@nd.edu
†Undergraduate Research Student, Department of Aerospace and Mechanical Engineering. jbruns2@nd.edu
‡Research Assistant Professor, Department of Aerospace and Mechanical Engineering. ajemcov@nd.edu

diffusion with a kinetic theory and demonstrated it provides a remedy for carbuncles. Chandrashkar [15] has formally returned to the Navier-Stokes model. Using an intricate hybrid numerical algorithm which introduces switches and a blending of other methods, coupled with sufficient numerical resolution, he has correctly removed carbuncles. A related hybrid method with similar complexities is reported by Nishikawa and Kitamura. [16] Kopriva [17] and later Hejranfar [18] give detailed discussion of viscous blunt body flows in the context of a problem in which the shock is fixed as an inflow boundary, thus precluding any carbuncle development; their results are validated against experimental results of Tewfik and Giedt [19] and can be compared to the Navier-Stokes solutions of Gnoffo. [20] Additional discussion in the context of a related problem is given by Druguet, et al. [21]

In this paper, we demonstrate a simpler antidote exists: introduction of physical momentum and energy diffusion via a simple discretization of the ordinary Navier-Stokes equations, employed on a sufficiently fine grid to capture viscous shocks. We demonstrate the carbuncle phenomenon and its rectification by solving two problems. Both employ the same geometry, initial conditions, computational grid, advective flux model of a Roe-based scheme without an entropy fix, and time-advancement scheme. For the first problem, we neglect physical diffusion, while for the second we include it. When physical diffusion is neglected, we predict a carbuncle phenomenon; however, when it is included and sufficiently resolved, no carbuncle is predicted, in agreement with experiment. Thus, we show that even a simple algorithm employing first order spatial and fourth order temporal discretizations, sufficiently resolved, fosters no carbuncle phenomena. In short, we use examples to support two hypotheses which are difficult to discern from the literature:

- *The carbuncle phenomenon, induced by many high resolution, nominally high order, shock-capturing schemes for Euler equations applied to supersonic flow over a blunt body, is cured by inclusion of properly resolved physical diffusion in a verified and validated Navier-Stokes model, and*
- *When fine scale physical diffusion structures are resolved, simple low order discretization schemes are sufficient to capture the continuum flow physics of supersonic flow over a blunt body.*

Our stratagem of reintroduction of physical diffusion gives a damping mechanism to suppress instabilities which we believe to be of numerical origin. Our model of physical diffusion is admittedly simple: a continuum model with constant properties. Such models induce shock waves of finite thickness with the thickness proportional to the diffusion parameters. As reviewed by Griffith and Bleakney, [22] experimental evidence exists for a continuum description of shock waves in gases; the continuum theory becomes increasingly accurate as the shock weakens. However, they note for $M > 1.2$ "continuous fluid theory may not give as satisfactory an interpretation as the kinetic theory of gases," and this notion is commonly used to discount continuum theories of shock structure in high Mach number environments. Other insist more emphatically, e.g. Li, *et al.,* [14] that continuum theories are "not valid" to predict shock structure in that only a small number of molecular collisions are likely within a shock, contrary to the continuum assumption.

Nevertheless, such statements are likely overly conservative for many purposes. As noted by Vincenti and Kruger, [23] "...comparisons with experiment show that the Navier-Stokes solution is accurate for larger values of [Mach number than] might be expected from purely theoretical considerations." They go on to note "It is sometimes said that the test of a good theory is whether its usefulness exceeds its expected range of validity; the Navier-Stokes equations amply satisfy this condition." An extensive discussion of viscous shock waves in the context of experiments, and supporting continuum and non-continuum theories can be found in Müller and Ruggeri, [24] where it is demonstrated that continuum theory actually predicts shock thickness well for an unexpectedly large range of freestream conditions, with surprisingly good agreement achieved for $1 < M < 11$. Visual inspection of their Fig. 12.2 shows the correct trends as M is varied, and a maximum validation error of $\sim 20\%$ near $M = 4$. More recent theoretical insights into viscous shock structure has been given by many sources including Myong [25] and Solovchuk and Sheu. [26]

II. Model

A. Mathematical model

Our general mathematical model, which we restrict to two spatial dimensions, is taken to be

$$\frac{\partial \rho}{\partial t} + \nabla \cdot (\rho \mathbf{u}) \quad = \quad 0, \tag{1}$$

$$\frac{\partial}{\partial t}(\rho \mathbf{u}) + \nabla \cdot \left(\rho \mathbf{u}\mathbf{u}^T\right) = -\nabla p + \nabla \cdot \boldsymbol{\tau}, \tag{2}$$

$$\frac{\partial}{\partial t}\left(e + \frac{1}{2}\mathbf{u}\cdot\mathbf{u}\right) + \nabla \cdot \left(\rho \mathbf{u}\left(e + \frac{1}{2}\mathbf{u}\cdot\mathbf{u}\right)\right) = -\nabla \cdot \mathbf{q} - \nabla\left(p\mathbf{u}\right) + \nabla \cdot \left(\boldsymbol{\tau}\cdot\mathbf{u}\right), \tag{3}$$

$$\mathbf{q} = -k\nabla T, \tag{4}$$

$$\boldsymbol{\tau} = 2\mu\left(\frac{\nabla\mathbf{u} + (\nabla\mathbf{u})^T}{2} - \frac{1}{3}(\nabla\cdot\mathbf{u})\mathbf{I}\right), \tag{5}$$

$$p = \rho R T, \tag{6}$$

$$e = c_v T. \tag{7}$$

Here Eqs. (1-3) represent the conservation of mass, linear momenta, and energy, respectively. Equations (4,5) are constitutive laws for energy and momenta diffusion which assume an isotropic material that obeys Fourier's law and a Newtonian stress-strain rate relation for a fluid which obeys Stokes' assumption. Equations (6,7) are thermal and caloric state equations for a calorically perfect ideal gas. The independent variables are time t, and the spatial Cartesian coordinates x and y. Dependent variables are density ρ, velocity vector $\mathbf{u}$, pressure p, viscous stress tensor $\boldsymbol{\tau}$, specific internal energy e, heat flux vector $\mathbf{q}$, and temperature T. We take $\mathbf{I}$ as the identity matrix. Constant parameters are thermal conductivity k, viscosity μ, gas constant R, and specific heat at constant volume c_v. The flow is initialized at the freestream values and thus simulates the introduction of a cylinder into an otherwise homogeneous flow at $t = 0$. For all calculations, zero gradient conditions are imposed at outflow boundaries. For viscous calculations, no-slip adiabatic boundary conditions are imposed at the cylinder surface. For inviscid calculations, a zero mass flux condition is imposed at the cylinder surface. The flow has known freestream properties $\mathbf{u}_1 = (u_1, 0)^T$, p_1, and T_1 and flows over a cylinder of radius a. Parameters which may be derived from the fundamental parameters include the ratio of specific heats $\gamma = 1 + R/c_v$, the freestream Mach number $M_1 = u_1/\sqrt{\gamma R T_1}$, the ambient sound speed, $c_1 = \sqrt{\gamma R T_1}$, the ambient density $\rho_1 = p_1/R/T_1$, and the ambient kinematic viscosity $\nu_1 = \mu/\rho_1$.

We choose the parameters listed in Table 1, which are appropriate for air. Two of the more important length scales in the problem are the viscous shock thickness and the cylinder radius. Both scales need to be resolved, and resolution becomes increasingly challenging as their ratio increases. Our choice of a low ambient pressure of 12.4272 Pa induces a shock thickness of a few microns, moderately smaller than our cylinder radius of 150 microns. A rough estimate of shock thickness λ can be inferred from Vincenti and Kruger, [23] showing $\lambda \sim \nu_1/c_1 = 17.19$ microns. This modest range of scales allows us to resolve all modeled physics in a reasonable computational time using ordinary single-processor resources. Had we chosen higher ambient pressures (thus inducing smaller shock thicknesses) and larger cylinders, the computational resources necessary for resolving the flow physics would become more demanding. Nearly all of our parameters are consistent with those employed by Kopriva [17] with the exception of cylinder radius, which was chosen to be smaller in order to reduce the computational costs. With our choices, we thus model a Prandtl number $Pr = \mu c_p/k = 0.77$ and Reynolds number, $Re = \rho_1 u_1 a/\mu = 50$.

B. Numerical method

All simulations were performed using the public domain software, OpenFOAM. [27] A typical calculation took about three hours on a four core laptop computer. The time-advancement scheme was a fourth-order Runge-Kutta method. The grids employed consisted of approximately 120,000 hexahedral finite volume cells. The horizontal extent of the domain is 0.0005377 m (537.7 microns). A typical cell length scale was 5.377 microns or smaller, sufficiently small to capture all the continuum flow features. The numerical scheme was of the Godunov type with the Roe flux difference splitting scheme used for the evaluation of the advective face fluxes. [28] The advective numerical scheme, which had nominal second order accuracy in space, was obtained by the linear cell-to-face interpolation utilizing the gradients of the primitive fields with a Barth-Jespersen limiter. [29] As with all shock-capturing schemes applied to Euler equations, the asymptotic convergence rate is less than unity. [30] For Navier-Stokes calculations, first order spatial discretization was employed on diffusive terms, and it is possible to achieve a consistent convergence rate when the grid is sufficiently fine to resolve the shock structure.

III. Results

Figure 1 shows the pressure field at $t = 2\times10^{-6}$ s when physical diffusion is neglected ($\mu = k = 0$). At this time the carbuncle has appeared within the solution. The region indicated within the green triangle attached to the cylinder surface is essentially the same carbuncle phenomenon predicted in other independent studies. It is noted that particularities of the carbuncle vary from study to study. There is slip on the cylinder surface and a crisp shock standing off from the surface. Detailed examination reveals that the inviscid shock jumps over approximately two cells. Figure 2 shows analogous predictions in the presence of physical diffusion. Clearly, there is no carbuncle.

In order to find the time in which the viscous shock has relaxed to a fixed state, the relative error of each Navier-Stokes solution on various grids is plotted with respect to time. Figure 3 shows the relative error of pressure at a point for three different runs with various grid sizes, using a very fine grid (having an average $\Delta x \approx 1 \times 10^{-6}$ m) as the "true" solution denoted by p_∞. The relative error was calculated at the same point for each run, a point located directly in front of the cylinder. The point is located at the coordinate $(-150.3 \times 10^{-6}$ m, 0 m, 0 m) if the origin is located at the center of the cylinder. From this plot, it is seen that the error has sufficiently relaxed at a time of $t = 5 \times 10^{-6}$ s. Figure 4 shows a plot of the relative error with respect to the grid size for the same three grids, using the relative error at $t = 5 \times 10^{-6}$ s. A least squares curve fit reveals that the solution is converging at $O(\Delta x^{1.38})$. It is anticipated that had finer grids been used, the solution would move into the asymptotic convergence regime in which the convergence rate was $O(\Delta x^1)$.

A simple validation is given by comparing our prediction of shock standoff distance against the curve-fit formula deduced from experimental data reported by Ambrosio and Wortman. [31] Their formula, $\Delta/a = 0.386\exp(4.67/M_1^2)$, where Δ is the standoff distance, results in $\Delta = 66.7\pm1$ microns. Our inviscid prediction, which includes the effect of the carbuncle, is $\Delta = 103.5 \pm 2$ microns; however, it is by no means clear that the carbuncle has relaxed to a steady state. Our viscous prediction is $\Delta = 41 \pm 2$ microns. Certainly the viscous approximation is good and agrees better with experiment than the inviscid approximation. The remaining discrepancies between the viscous approximation and the experiment might be attributable to either the finite domain size or more likely other neglected physics, such as temperature-dependent specific heat, viscosity, and thermal conductivity, as well as real gas effects.

IV. Discussion

We note that our remedy of resolving physical viscous shocks is impractical given present computational resources for problems involving devices with the larger geometries and higher pressures encountered in typical aerospace engineering applications. An imperfect compromise which also should avoid the carbuncle phenomenon could be achieved by introducing an artificial strain rate dependency into the viscosity coefficient in a tensorially invariant fashion that is guaranteed to satisfy a Clausius-Duhem inequality and allow resolution of enhanced shock thicknesses by ordinary numerical methods. A similar strategy has been employed in a different context by Bhagatwala and Lele. [32] This approach however runs the risk of artificially filtering high frequency phenomena which have a physical origin, such as in acoustics, shock-boundary layer instabilities, or combustion instabilities. Whatever the ultimate approach one takes to engineering problems, there is always value to fully resolved benchmarking exercises which resolve a broad range of the actual multi-scale physics without resort to artificial viscosity.

V. Conclusions

In summary, when a simple physical diffusion model is introduced into the model of fluid motion and its effects simulated on a sufficiently fine grid, the carbuncle phenomenon is removed. We speculate that the carbuncle may arise due to what amounts to what is sometimes called "anti-diffusion," an effect which has been shown to exist via construction of the so-called "modified equation" for many shock-capturing schemes when exercised on Euler equations; see Banks, et al. [30]

Acknowledgments

This work was performed under support of the Center for Undergraduate Scholarly Engagement at the University of Notre Dame. The authors thank Dr. K. Shi of University of Notre Dame for her help in mesh generation and post-processing of data.

References

[1]Peery, K. M., and Imlay, S. T., "Blunt Body Flow Simulations," AIAA Paper 88-2924, July 1988.

[2]Quirk, J. J., "A Contribution to the Great Riemann Solver Debate," *International Journal for Numerical Methods in Fluids*, Vol. 18, No. 6, 1994, pp. 555-574.

[3]Robinet, J. C., Gressier, J., Casalis, G., and Moschetta, J. M., "Shock Wave Instability and the Carbuncle Phenomenon: Same Intrinsic Origin?," *Journal of Fluid Mechanics*, Vol. 417, 2000, pp. 237-263.

[4]Srinivasan, B., Jameson, A., and Krishnamoorthy, S. "An Upwinded State Approximate Riemann Solver," *International Journal for Numerical Methods in Fluids*, Vol. 70, No. 5, 2012, pp. 578-602.

[5]Kitamura K., Shima, E., and Roe, P. L., "Carbuncle Phenomena and Other Shock Anomalies in Three Dimensions," *AIAA Journal*, Vol. 50, No. 12, 2012, pp. 2655-2669.

[6]MacCormack, R. W., "Carbuncle Computational Fluid Dynamics Problem for Blunt-Body Flows," *Journal of Aerospace Information Systems*, Vol. 10, No. 5, 2013, pp. 229-239.

[7]Dumbser, M., Moschetta, J.-M., and Gressier, J., "A Matrix Stability Analysis of the Carbuncle Phenomenon," *Journal of Computational Physics*, Vol. 197, No. 2, 2004, pp. 647-670.

[8]Chauvat, Y., Moschetta, J.-M., and Gressier, J., "Shock Wave Numerical Structure and the Carbuncle Phenomenon," *International Journal for Numerical Methods in Fluids*, Vol. 47, Nos. 8-9, 2005, pp. 903-909.

[9]Elling, V., "The Carbuncle Phenomenon is Incurable," *Acta Mathematica Scientia*, Vol. 29, No. 6, 2009, pp. 1647-1656.

[10]Pandolfi, M., and D'Ambrosio, D., "Numerical Instabilities in Upwind Methods: Analysis and Cures for the 'Carbuncle' Phenomenon," *Journal of Computational Physics*, Vol. 166, No. 2, 2001, pp. 271-301.

[11]Ismail, F., Roe, P. L., and Nishikawa, H., "A Proposed Cure to the Carbuncle Phenomenon," *Computational Fluid Dynamics 2006: Proceedings of the Fourth International Conference on Computational Fluid Dynamics, ICCFD4*, edited by H. Deconnick and E. Dick, Springer, Berlin 2009, pp. 149-154.

[12]Liou, M.-S., "Mass Flux Schemes and Connection to Shock Instability," *Journal of Computational Physics*, Vol. 160, No. 2, 2000, pp. 623-648.

[13]Ohwada, T., Adachi, R., Xu, K., and Luo, J., "On the Remedy Against Shock Anomalies in Kinetic Schemes," *Journal of Computational Physics*, Vol. 255, 2013, pp. 106-129.

[14]Li, J., Li, Q., and Xu, K., "Comparison of the Generalized Riemann Solver and the Gas-Kinetic Scheme for Inviscid Compressible Flow Simulations," *Journal of Computational Physics*, Vol. 230, No. 12, 2011, pp. 5080-5099.

[15]Chandrashekar, P., "Kinetic Energy Preserving and Entropy Stable Finite Volume Schemes for Compressible Euler and Navier-Stokes Equations," *Communications in Computational Physics*, Vol. 14, No. 5, 2013, pp. 1252-1286.

[16]Nishikawa, H., and Kitamura, K., "Very Simple, Carbuncle-Free, Boundary-Layer Resolving Rotated-Hybrid Riemann Solvers, *Journal of Computational Physics*, Vol. 227, No. 4, 2008, pp. 2560-2581.

[17]Kopriva, D. A., "Spectral Solution of the Viscous Blunt-Body Problem," *AIAA Journal*, Vol. 31, No. 7, 1993, pp. 1235-1242.

[18]Hejranfar, K., Esfahanian, V., and Najafi, M., "On the Outflow Conditions for Spectral Solution of the Viscous Blunt-Body Problem," *Journal of Computatoinal Physics*, Vol. 228, No. 11, 2009, pp. 3936-3972.

[19]Tewfik, O. K., and Giedt, W. H., "Heat Transfer, Recovery Factor, and Pressure Distributions Around a Circular Cylinder Normal to a Supersonic Rarefied-Air Stream," *Journal of the Aerospace Sciences*, Vol. 27, No. 10, 1960, pp. 721-729.

[20]Gnoffo, P. A., "Complete Supersonic Flowfields over Blunt Bodies in a Generalized Orthogonal Coordinate System," *AIAA Journal*, Vol. 18, No. 6, 1980, pp. 611-612.

[21]Druguet, M.-C., Candler, G. V., and Nompelis, I., "Effect of Numerics on Navier-Stokes Computations of Hypersonic Double-Cone Flows," *AIAA Journal*, Vol. 43, No. 3, 2005, pp. 616-623.

[22]Griffith, W. C., and Bleakney, W., "Shock Waves in Gases," *American Journal of Physics*, Vol. 22, No. 9, 1954, pp. 597-612.

[23]Vincenti, W. G., and Kruger, C. H., *Introduction to Physical Gas Dynamics*, John Wiley, New York, 1965, p. 415.

[24]Müller, I., and Ruggeri, T., *Rational Extended Thermodynamics, Second Edition*, Springer, New York, 1998, pp. 277-308.

[25]Myong, R. S., "Analytical Solutions of Shock Structure Thickness and Asymmetry in Navier-Stokes/Fourier Framework," *AIAA Journal*, Vol. 52, No. 5, 2014, pp. 1075-1080.

[26]Solovchuk, M. A., and Sheu, T. W. H., "Prediction of Shock Structure Using the Bimodal Distribution Function," *Physical Review E*, Vol. 81, No. 5, 2010, 056314.

[27]Jasak, H., Jemcov, A., and Tuković, Ž., "OpenFOAM: A C++ Library for Complex Physics Simulations", *International Workshop on Coupled Methods in Numerical Dynamics*, IUC, Dubrovnik, Croatia, September 2007.

[28]Roe, P. L., "Approximate Riemann Solvers, Parameter Vectors, and Difference Schemes", *Journal of Computational Physics"*, Vol. 43, No. 2, 1981, pp. 357-372.

[29]Barth, T. J., and Jespersen, D. C., "The Design and Application of Upwind Schemes on Unstructured Meshes", AIAA Paper 89-0366, January 1989.

[30]Banks, J. W., Aslam, T., and Rider, W. J., "On Sub-Linear Convergence for Linearly Degenerate Waves in Capturing Schemes," *Journal of Computational Physics*, Vol. 227, No. 14, 2008, pp. 6985-7002.

[31]Ambrosio, A., and Wortman, A., "Stagnation Point Shock Detachment Distance for Flow Around Spheres and Cylinders," *ARS Journal*, Vol. 32, No. 2, 1962, p. 281.

[32]Bhagatwala, A., and Lele, S. K., "A Modified Artificial Viscosity Approach for Compressible Turbulence Simulations, *Journal of Computational Physics*, Vol. 228, No. 14, 2009, pp. 4965-4969.

Table 1. Parameter values for Navier-Stokes simulations of flow over a cylinder.

parameter	value	units
R	287.7	J/kg/K
c_v	719.3	J/kg/K
c_p	1007	J/kg/K
p_1	12.4272	Pa
T_1	39.667	K
u_1	724.293	m/s
M_1	5.73	
γ	7/5	
μ	2.3648×10^{-6}	Pa s
k	0.003093	W/m/K
a	0.00015	m
ρ_1	0.001088	kg/m^3
c_1	126.404	m/s
ν_1	0.002174	m^2/s
Re	50	
Pr	0.77	

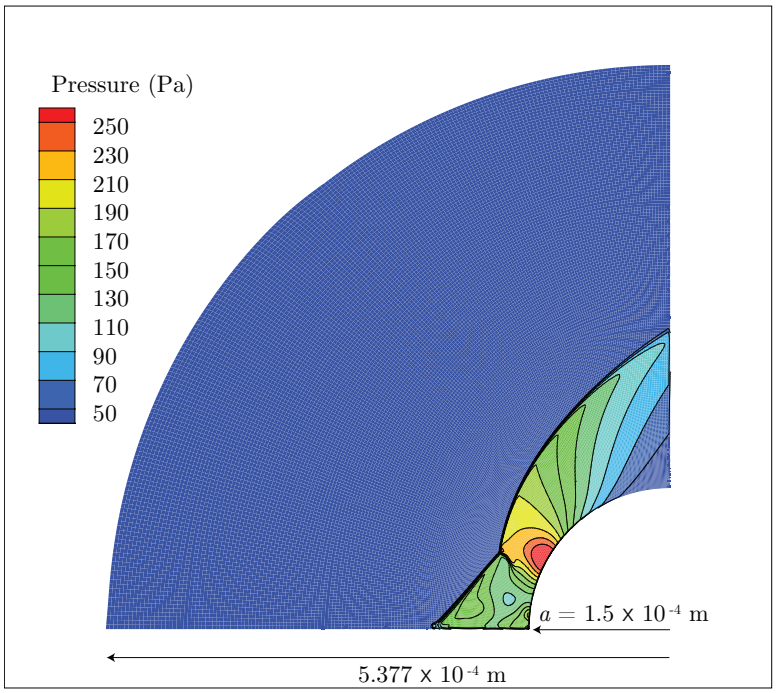

Figure 1: Detail of pressure field with physical diffusion neglected.

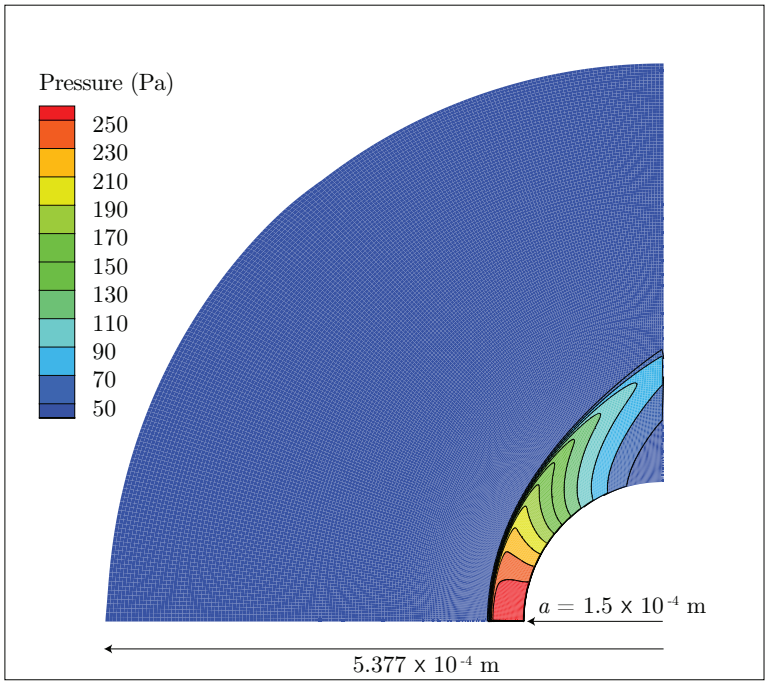

Figure 2: Detail of pressure field with physical diffusion.

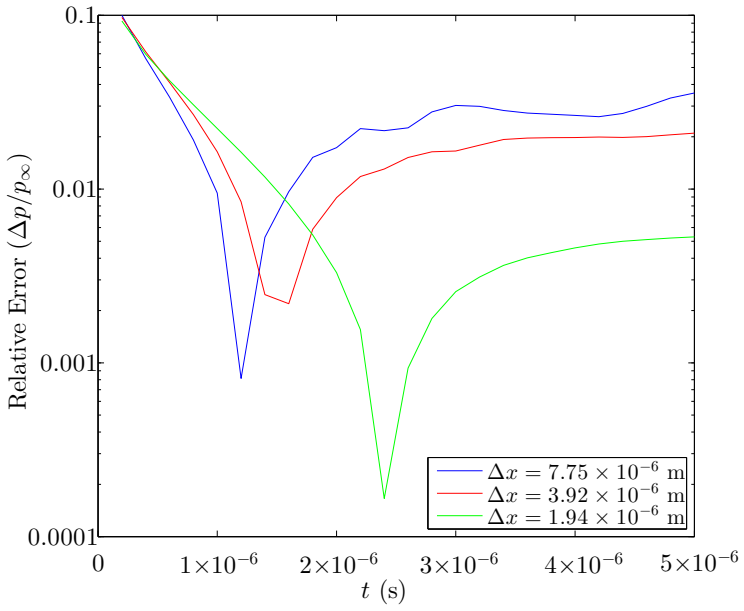

Figure 3: Relative error of the pressure at a single point with respect to time for three different grid resolutions.

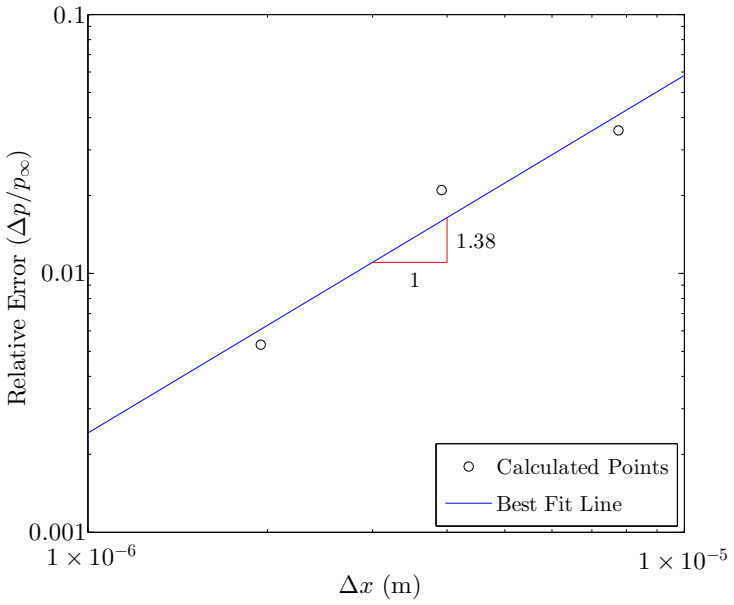

Figure 4: Relative error of the pressure at a single point as a function of Δx for three different grid resolutions.